Springer

KSME

Journal of Mechanical Science and Technology 32 (9) (2018) 4223~4229
www.springerlink.com/content/1738-494x(Print)/1976-3824(Online)
DOI 10.1007/s12206-018-0820-6

Experimental investigation of the preferred Strouhal number used in self-resonating pulsed waterjet †

Deng Li[1,2], Youping Chen[1,*], Yong Kang[2], Zu'an Wang[2], Xiaoliang Wang[2], Qi Fan[2] and Miao Yuan[2]

[1]*School of Mechanical Science and Engineering, Huazhong University of Science and Technology, Wuhan 430074, Hubei Province, China*
[2]*School of Power and Mechanical Engineering, Wuhan University, Wuhan 430072, Hubei Province, China*

(Manuscript Received January 11, 2018; Revised May 11, 2018; Accepted May 22, 2018)

Abstract

Self-resonating pulsed waterjet (SRPW) is superior to plain waterjet in many ways and is being employed in numerous applications. To further improve the performance of SRPW, the optimal value of the preferred Strouhal number (S_d), which is used to determine the chamber length of a self-resonating nozzle, was experimentally studied at inlet pressures of 10 MPa and 20 MPa. The axial pressure oscillation peak and amplitude were used to evaluate the performance of SRPW, in order to find the optimum S_d value. Results show that S_d value determines the self-resonance behavior of an organ-pipe nozzle and greatly affects the intensity of the axial pressure oscillation. Under the experimental conditions, the optimum S_d values are 0.315 and 0.278 respectively, corresponding to inlet pressures of 10 MPa and 20 MPa. Compared with the default value of 0.3 obtained from air jet experiment, the optimum S_d value at inlet pressure of 10 MPa is a little larger and oppositely a bit smaller at inlet pressure of 20 MPa. Thus, if the inlet pressure is not considered, S_d value of 0.3 is reasonable for determining the chamber length of a self-resonating nozzle for generating effective SRPW.

Keywords: Strouhal number; Self-resonating waterjet; Pressure oscillation; Organ-pipe nozzle

1. Introduction

Due to the outstanding advantages of high pressure waterjet (HPW) such as no heat-affected zone, low cost, and environmentally friendly, it has been considered as a promising technology that can be employed in many areas [1-5]. For example, Huang et al. [2] used HPW to remove heat-formed coating from a titanium alloy and found this technology is capable for the removal of such hard and difficult-to-machine coatings. Through an exploratory experimental investigation, Careddu and Akkoyun [3] demonstrated that HPW can be used for efficient graffiti cleaning with specific operational conditions. Moreover, Jiang et al. [4] used HPW for dust suppression in coal mines and found the dust concentration could be reduced by over 90 % on average when waterjet was used during rock cutting. And in the medical field, Dunnen et al. [5] claimed that HPW drilling provides several advantages over classic drilling with rigid drilling bits in orthopedic surgery.

With the rapid development of HPW technology, new types of waterjet like cavitating waterjet, abrasive waterjet, and self-resonating pulsed waterjet have been put forward and studied in order to meet the demand for more powerful erosion ability without increasing the pump pressure [6-8]. And among these novel waterjets, SRPW has been especially focused after being proposed by Johnson et al. [9].

SRPW is a newly proposed novel waterjet that can be yielded with the use of specially structured nozzles. To be more specific, by using a suitable self-resonating chamber, the turbulent shear layer of a HPW can be amplified and structured and the jet can be passively disrupted, leading to the generation of a train of discrete water slugs. Then these water slugs produce high-frequency and high pressure shock wave impacts able to enhance the erosion capability and working efficiency of the jet. On the other hand, SRPW also has very high amplitude, periodic, and oscillatory discharge without using moving parts in the supply system, which helps eliminate the cushion effect and improve the performance. In other words, SRPW is a totally acoustically generated jet that takes advantage of the natural tendency of an axisymmetric turbulent jet to organize into large-scale structures [10]. Therefore, SRPW efficiently avoids the drawbacks of mechanically generated pulsed waterjet like, high-levels of mechanical maintenance, high cost, limited durability in harsh environment, and short life-times [11].

Because of the foregoing unique advantages of SRPW, it has been regarded as one of the most promising novel waterjets and has been the subject of a relative intense research

*Corresponding author. Tel.: +86 2768774906, Fax.: +86 2768774906
E-mail address: 2008lee@whu.edu.cn
† Recommended by Associate Editor Sangyoup Lee

effort in the literature. In more specific terms, Yoshikawa et al. [12] carried out an experiment to examine the vortex-sound generation process happening in an organ-pipe and proposed a vortex-layer formation model to provide a united viewpoint for the edge-tone generation. To improve the exploration and production of petroleum, Wang et al. [13] applied self-resonance concept in the drilling method and came up with a self-excited pulsed jet drilling technology. Moreover, Arthurs and Ziada [14] experimentally studied the influence of thickness of nozzle exit on self-excited impinging jet and concluded that jet oscillation is controlled by a fluid-dynamic mechanism for small impinge distances. Indeed, our research team has also conducted a series of experimental and numerical investigations on SRPW, from feeding pipe diameter to surface roughness [15-25].

Even the generation mechanism and new applications of SRPW have been greatly studied, the value of the preferred Strouhal number, S_d, however does not appear to be adequately treated in the literature. As is known to all, Stouhal number, S_t, is a dimensionless number describing oscillating flow mechanism and is particularly important in studying self-excited or self-sustained oscillations. In the mechanism study of SRPW, Johnson et al. [9] established an equation for estimating the ratio of chamber length to jet diameter based on empirical acoustic analysis, in order to get an effective self-resonating nozzle. According to the research of self-sustained air jet carried out by Crow and Champagne [26], $S_d = 0.3$ was used in the equation. And the same value was also used in the design of organ-pipe resonating nozzles by Li et al. [27], who employed SRPW in China oil field. However, as is well-known, air jet is much different from waterjet, and $S_d = 0.3$ obtained in the air jet experiment may not satisfy the self-excited waterjet. So far, to the best of our knowledge, there is currently very little literature on this.

The present study provides an experimental investigation on the pressure oscillation characteristics of SRPW issuing from organ-pipe nozzles of different chamber lengths, in order to obtain the optimum S_d values for determining the nozzle structures under different working pressures. As a continuation of our previous research [15-25] on SRPW, this study also helps make a contribution to improving the working efficiency of SRPW.

2. Strouhal number in SRPW

In order to show the importance of S_t in SRPW, a brief description of the operating principles of the jet discharging from an organ-pipe nozzle is presented as follows.

As is depicted in Fig. 1, the typical self-resonating organ-pipe nozzle consists two area contractions, defined by $(D_i/D_c)^2$ and $(D_c/D_e)^2$, and a resonance chamber of diameter of D_c and length of L_c. Pressure waves will be generated at the downstream contraction if a flow is rapidly passing though the nozzle. The waves propagating upwards are then reflected by the upstream contraction and superimpose with the original ones.

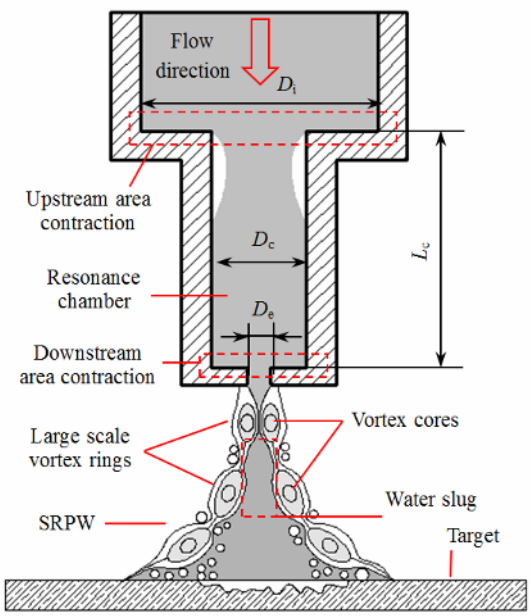

Fig. 1. Schematic of the working principles of SRPW.

And a standing wave will be formed in the resonance chamber if the fundamental frequency (f_0) of the nozzle meets the main frequency (f_v) of the strongest pressure wave. The standing wave is capable of structuring the shear layer of the jet into large scale vortex rings, resulting in large pressure oscillations of the jet and finally the emergence of SRPW. More detail information of the generation mechanism of SRPW can be found in Refs. [9, 10, 16, 17, 20-24].

Furthermore, it is well-known that f_0 is determined by chamber length L_c and can be expressed as:

$$f_0 = K_n \frac{c}{L_c} \tag{1}$$

where c is local sound speed, K_n is model number.

And f_v can be expressed with the use of S_t:

$$f_v = \frac{S_t U_e}{D_e} \tag{2}$$

where U_e is the jet velocity, and here jet diameter has been equal to the exit diameter D_e for the sake of simplicity.

To get an effective SRPW, the two frequencies should be equal, which leads to the following equation:

$$f_0 = f_v \Rightarrow \frac{L_c}{D_e} = \frac{K_n c}{U_e S_d}. \tag{3}$$

Therefore, once D_e is given, L_c can be obtained by the value of S_d. In other words, the value of S_d determines the effectiveness of the self-resonating organ-pipe nozzle and further the performance of SRPW.

Even S_d is dramatically important in determining the struc-

ture parameter (L_c) of an organ-pipe nozzle, there is currently very little literature on verifying the accuracy of S_d = 0.3 for SRPW. And this study is trying to provide an experimental attempt to figure out this problem.

3. Experimental setup and procedures

3.1 Facilities and setup

Since the axial pressure oscillation peak and amplitude are among the most distinct characteristics of SPRW [9, 10, 16-24], these were used to evaluate the performance. Therefore, the axial pressure measurement experiment was performed.

Fig. 2 presents a schematic diagram of the experimental setup. The experiment was carried out on a multifunctional waterjet test bed that had been used in our previous study [15-25]. The test bed had a horizontal moving table with X-direction movement and a loading platform with Y-direction and Z-direction movements. High pressure water was provided by a plunger pump whose maximum working pressure and flow rate were 60 MPa and 120 L/min, respectively. The movements and the pump pressure could be regulated by the control table. The temperature of the tap water was 20 °C, consistent with that of the environment.

To minimize the flow rate and pressure disturbances, two bladder accumulators were employed in the system with one positioned near the pump and the other close to the testing nozzle, shown in Fig. 2.

A static pressure transducer (Model: BD Sensors DMK331P) was located as closely as possible to the entrance of the nozzle to get the inlet pressure (P_i) for each test. During each test, SRPW impinged on a target plate with a 1 mm diameter hole located at its center. A dynamic pressure transducer (Model: XPM10) communicating with the pressure tap was mounted on the wall of the tank, so as to obtain the time-resolved axial pressure of the jet. The test results were then acquired by the data logger (Model: MX840B) connected with a laptop. And the maximum and minimum pressures (P_{max} and P_{min}) could be directly obtained from the laptop. The main parameters of the transducers are shown in the following tables.

Standoff distance, S, was defined as the distance between the exit of the nozzle and the surface of the target plate. Various standoff distances from 10 mm to 100 mm with an interval of 10 mm were applied during each test.

3.2 Organ-pipe nozzles design

Based on Eq. (3), it can be found that U_e should be given to get the relation between L_c and S_d. In order to verify the rea-

Table 1. Main parameters of the static pressure transducer.

Model	Parameter	Value
BD DMK331P	Nominal pressure/MPa	40
	Burst pressure/MPa	100
	Accuracy	≤ ±0.5 %FS
	Influence effects of supply/10 V	0.05 %FS
	Influence effects of load/kΩ	0.05 %
	Thermal error/10 K	±0.5 %FS

Table 2. Main parameters of the dynamic pressure transducer.

Model	Parameter	Value
XPM 10	Nominal pressure/MPa	35
	Burst pressure/MPa	105
	Frequency response/KHz	288
	Accuracy	≤ ±0.25 %FS
	Repeatability	±0.2 %
	Nonlinearity	±0.25 %

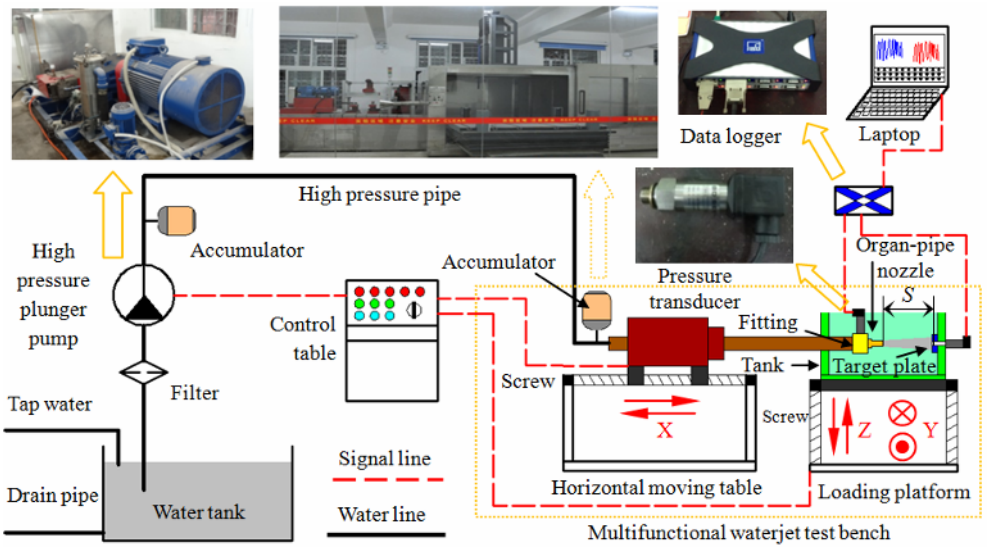

Fig. 2. Schematic diagram of the experimental setup for the pressure tests.

Table 3. Parameters of organ-pipe nozzles and corresponding values of S_d.

P_i/MPa	L_c/mm, S_d							D_i/mm	D_c/mm	D_e/mm	L_e/mm
10	18	19	20	21	22	23	24	13	5	2	5
	0.35	0.33	0.315	0.3	0.286	0.27	0.26				
20	12	13	14	15	16	17	18				
	0.37	0.34	0.318	0.3	0.278	0.262	0.25				

sonability of S_d = 0.3 and find the optimal value, different chamber lengths were used to get different S_d values. And it should be emphasized that organ-pipe nozzle has two abrupt area contractions, the energy loss under high pressure condition is relatively large and cannot be neglected. So, the process for calculating U_e is shown below:

The Bernouli equation gives the express of U_e:

$$\frac{P_i}{\rho g}+\frac{U_i^2}{2g}=\frac{P_a}{\rho g}+\frac{U_e^2}{2g}+h_f+h_j \tag{4}$$

where P_i is inlet pressure, ρ is the liquid density, g is the acceleration of gravity, h_f is the frictional head loss, h_j is the local head loss. And h_f and h_j can be written as:

$$h_f=\lambda\frac{l}{d}\frac{u^2}{2g} \tag{5}$$

$$h_j=k\frac{u^2}{2g} \tag{6}$$

where λ is the friction coefficient, l is the length of the flow channel (here it is the nozzle length), d is channel diameter, u is flow velocity, and k is the local resistance coefficient. Under the sudden contraction condition, k can be expressed as:

$$k=\frac{1}{2}\left(1-\left(\frac{A_2}{A_1}\right)^2\right)^2 \tag{7}$$

where A_1 and A_2 are the cross-section areas at the contraction.

In Eq. (5), λ, l and u are rather small. So, it can be neglected during the calculation. When compared with U_e, U_i can also be neglected.

Then, based on the experimental results obtained by Li et al. [27], the structure parameters of the organ-pipe nozzles used in this experiment could be achived by combining Eqs. (3), (4), (6) and (7). It should be noticed that during the calculation, S_d = 0.3 was first assumed reasonable, as this value has already been used in many previous investigations [9, 10, 16-24]. After the resulted optimal L_c was obtained, six another lengths next to it were used to get the corresponding S_d values, shown in Table 3. And the pictures of the nozzles are shown in Fig. 3.

4. Results and discussion

The performance of SRPW, which could be characterized by the axial pressure oscillation peak (P_{max}) and amplitude (P_a), was used to evaluate the optimal value of S_d. And P_a was defined as the difference between P_{max} and P_{min}.

Fig. 3. Pictures of the organ-pipe nozzles.

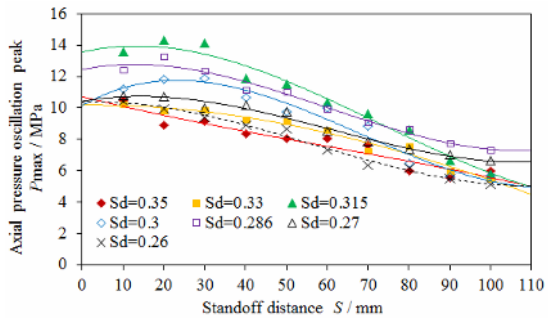

(a)

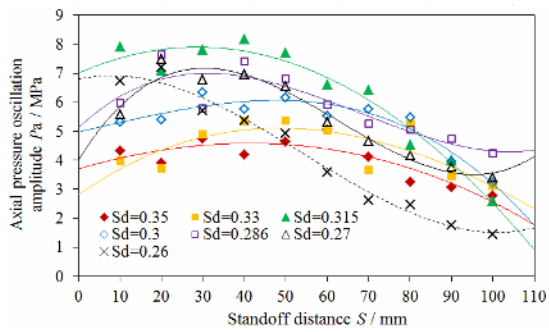

(b)

Fig. 4. Axial pressure oscillation peak (a); amplitude (b) against standoff distance at P_i = 10 MPa.

4.1 Effects of the value of S_d at P_i = 10 MPa

Fig. 4 is the axial pressure oscillation peak and amplitude of SRPW against standoff distance with respect to various S_d values under inlet pressure of 10 MPa. As can be observed in

the figure, the value of S_d greatly affects the pressure oscillations, especially the amplitude, because the curves are more scattered with each other compared with the situation of pressure oscillation peak.

Specifically, within the range of $0.27 < S_d < 0.33$, the pressure oscillation peak first gradually goes up and then drops gently with the increase of standoff distance, shown in Fig. 4(a). At standoff distance around 20 mm, which is defined as optimum standoff distance, the pressure oscillation peak reaches to its maximum. These are unique features of SRPW and are in good agreement with the previous study [9, 17, 21, 23]. On the other hand, when the value of S_d is out of the range, the pressure oscillation peak almost linearly decreases with standoff distance, indicating that the jet is losing self-resonance feature and seems to be transforming to a regular waterjet. And the pressure oscillation peak can hardly exceed the inlet pressure. Therefore, it can be expected that there is a specific rage for the value of S_d in order to generate obvious pressure oscillation peaks and effective SRPWs.

For the pressure oscillation amplitude shown in Fig. 4(b), it first increases and then decreases with the increase of standoff distance for almost all S_d values. There also exists an optimum standoff distance for achieving the maximum pressure oscillation amplitude. And this optimum standoff distance is about 10 mm larger than that for the maximum pressure oscillation peak. Besides, S_d values of 0.35 and 0.33 both lead to relatively smaller pressure oscillation amplitudes within the testing standoff distance. Even 0.26 is the smallest value in this experiment, the pressure oscillation amplitude experiences a rapid decrease with increasing standoff distance. Contrary to the pressure oscillation peak under S_d = 0.26 condition, the pressure oscillation amplitude is abnormally relatively larger at standoff distances less than 50 mm. And based on the previous study [17, 21, 23], this should not be the feature of SRPW. However, due to the very limited research on the value of S_d in SRPW, this phenomenon can hardly be clearly explained at the current stage.

In general, under the condition of S_d = 0.315, the axial pressure oscillation is more violent than any other case with respect to larger pressure oscillation peaks and amplitudes. This indicates that 0.315, which is a little larger than the commonly used value achieved from air jet, should be the optimal value at inlet pressure of 10 MPa.

4.2 Effects of the value of S_d at P_i = 20 MPa

Fig. 5 shows the axial pressure oscillation peak and amplitude against standoff distance at inlet pressure of 20 MPa under the condition of various S_d values. It is obvious that the value of S_d plays an important role in affecting the performance of SRPW, and a suitable value can greatly intensify the axial pressure oscillation, especially for the pressure oscillation amplitude at relatively larger standoff distances.

For the pressure oscillation peak illustrated in Fig. 5(a), it has the unique feature of SRPW only at S_d values of 0.318, 0.3

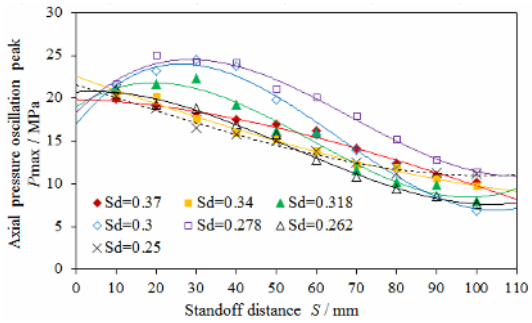

(a)

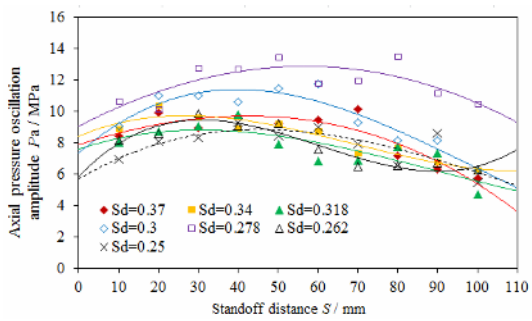

(b)

Fig. 5. Axial pressure oscillation peak (a); amplitude (b) against standoff distance at P_i = 20 MPa.

and 0.278. While in the other cases, the pressure oscillation peak decreases with increasing standoff distance and is more like the feature of a traditional submerged turbulent jet at relatively larger standoff distances. It should be noticed when the value is larger than 0.318 or smaller than 0.278, the cures are almost overlapped in the testing standoff distance, meaning the jets have nearly the same features. This also indicates that the nozzles have little self-resonance behavior and thus, the value of S_d hardly affects the axial pressure characteristics. Furthermore, the optimum standoff distance here is about 10 mm larger than that under inlet pressure of 10 MPa, which is in consistent with the previous study [16-24] and can be evidence for the reasonability of the experimental results.

When it comes to the pressure oscillation amplitude shown in Fig. 5(b), it is found that S_d values of 0.3 and 0.278 result in relatively larger amplitudes compared with the other cases. In addition, the optimum standoff distances are obviously larger than the corresponding ones for the pressure oscillation peak. Except for two values of 0.3 and 0.278, the overlap of the curves of the other values indicates the pressure oscillation amplitude is more sensitive to the value of S_d at higher inlet pressures. Because S_d value of 0.318 affects the pressure oscillation peak more obviously.

Generally, as can be observed in Fig. 5, S_d value of 0.278 should be the optimum at inlet pressure of 20 MPa, and both the pressure oscillation peak and amplitude are superior to the others under the experimental conditions. This also means the commonly used value of 0.3 is a little larger than the optimum value in this experiment.

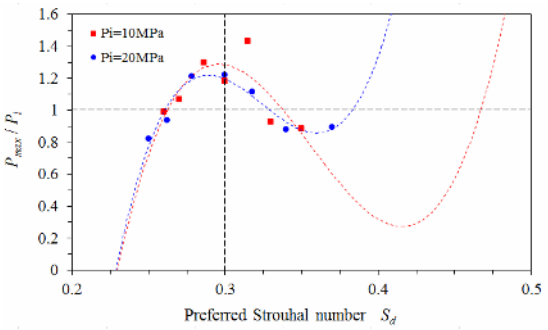

Fig. 6. Non-dimensional axial pressure oscillation peak as a function of the preferred Strouhal number at S = 20 mm for P_i = 10 MPa and S = 30 mm for P_i = 20 MPa.

4.3 Non-dimensional analysis

To further analyze the effects of S_d value on the performance of SRPW, the pressure oscillation peak has been non-dimensionalized by the inlet pressure. And the dimensionless pressure as a function of S_d under inlet pressures of 10 MPa and 20 MPa is plotted in Fig. 6. The pressure oscillation peaks at S = 20 mm and S = 30 mm for the two inlet pressures were used to analyze the effects. Moreover, cubic trend lines are added in the figure as well, in order to predict the effects of S_d values beyond the experimental ones.

As is shown in the figure, the axial pressure oscillation peak larger than the inlet pressure occurs in a small range of 0.27 < S_d < 0.32. And the dots distribute on both sides of the line of S_d = 0.3, which indicates that this value could be the most suitable one for achieving higher pressure oscillation peaks without taking the inlet pressure into consideration. From this point of view, the use of S_d = 0.3 in the previous study conducted by the pioneering researchers should be reasonable. And from the trendlines shown in the figure, it can be noticed that the pressure oscillation peak has a second increase when S_d value reaches to a certain range. Specifically, when S_d >0.4, the pressure oscillation peaks starts to rise under P_i = 10 MPa, while this value is 0.47 for the case of P_i = 20 MPa. If the experimental results obtained by Johnson et al. [9, 10] are taken into account, this can be explained by the mode number shown in Eq. (2). And from their results, all integer times of 0.3 can create self-resonance, but the intensities are different. Therefore, this also provides evidence for the reasonability of the experimental results.

However, it should be addressed that due to the rather limited literature on this aspect, this is a preliminary study on the effects of S_d values on the performance of SRPW, and the discussion is somewhat prospective. Further investigations with the use of mathematic and quantitative methods should be performed.

5. Conclusions

(1) The value of S_d greatly determines the axial pressure oscillation peak and amplitude of SRPW, a suitable value can obviously enhance the performance of the jet.

(2) At inlet pressure of 10 MPa, waterjet has the features of typical SRPW only when the value is within the range of 0.27 < S_d < 0.33. And 0.315 is the optimum value for obtaining the maximum pressure oscillation peaks and amplitudes at the optimum standoff distances.

(3) When the inlet pressure is 20 MPa, the nozzles will become regular ones without self-resonance behavior under the experimental conditions if S_d value does not locate in the rage of 0.278 < S_d < 0.318. And 0.278 is superior to 0.3 for intensifying the oscillation.

(4) In general, S_d = 0.3 is reasonable to be used for guiding the fabrication of self-resonating nozzles if the inlet pressure is not considered.

Acknowledgments

This research is financially supported by the National Key Basic Research Program of China (No. 2014CB239203) and China Postdoctoral Science Foundation Founded Project (No. 2017M620313).

References

[1] X. Liu, S. Liu and H. Ji, Mechanism of rock breaking by pick assisted with water jet of different modes, *Journal of Mechanical Science and Technology*, 29 (12) (2015) 5359-5368.

[2] L. Huang, P. Kinnell and P. H. Shipway, Removal of heat-formed coating from a titanium alloy using high pressure waterjet: Influence of machining parameters on surface texture and residual stress, *Journal of Materials Processing Technology*, 223 (4-5) (2015) 129-138.

[3] N. Careddu and O. Akkoyun, An investigation on the efficiency of water-jet technology for graffiti cleaning, *Journal of Cultural Heritage*, 19 (2016) 426-434.

[4] H. Jiang, C. Du and J. Dong, Investigation of rock cutting dust formation and suppression using water jets during mining, *Powder Technology*, 307 (2017) 99-108.

[5] S. den Dunnen, J. Dankelman, G. M. Kerkhoffs and G. Tuijthof, Colliding jets provide depth control for water jetting in bone tissue, *Journal of the Mechanical Behavior of Biomedical Materials*, 72 (2017) 219-228.

[6] S. T. Kumaran, T. J. Ko, R. Kurniawan, C. Li and M. Uthayakumar, ANFIS modeling of surface roughness in abrasive waterjet machining of carbon fiber reinforced plastics, *Journal of Mechanical Science and Technology*, 31 (8) (2017) 3949-3954.

[7] M. Santhanakumar, R. Adalarasan and M. Rajmohan, Parameter design for cut surface characteristics in abrasive waterjet cutting of Al/SiC/Al_2O_3, composite using grey theory based RSM, *Journal of Mechanical Science and Technology*, 30 (1) (2016) 371-379.

[8] N. Fujisawa, T. Kikuchi, K. Fujisawa and T. Yamagata, Time-resolved observations of pit formation and cloud be-

havior in cavitating jet, *Wear*, 386-387 (2017) 99-105.
[9] V. E. Johnson, W. T. Lindenmuth, A. F. Conn and G. S. Frederick, Feasibility study of tuned-resonator, pulsating cavitating water jet for deep-hole drilling, *No. SAND-81-7126*, Sandia National Labs., Albuquerque, NM (USA); Hydronautics, Inc., Laurel, MD, USA (1981).
[10] G. L. Chahine and V. E. Johnson, Mechanics and applications of self-resonating cavitating jets, *International Symposium on Jets and Cavities,* ASME, WAM (1985) 21-33.
[11] D. Hu, X. Li, C. Tang and Y. Kang, Analytical and experimental investigations of the pulsed air-water jet, *Journal of Fluids and Structures*, 54 (2015) 88-102.
[12] S. Yoshikawa, H. Tashiro and Y. Sakamoto, Experimental examination of vortex-sound generation in an organ pipe: A proposal of jet vortex-layer formation model, *Journal of Sound and Vibration*, 331 (11) (2012) 2558-2577.
[13] R. Wang, Y. Du, H. Ni and M. Lin, Hydrodynamic analysis of suck-in pulsed jet in well drilling, *Journal of Hydrodynamics, Ser. B*, 23 (1) (2011) 34-41.
[14] D. Arthurs and S. Ziada, Effect of nozzle thickness on the self-excited impinging planar jet, *Journal of Fluids and Structures*, 44 (2014) 1-16.
[15] W. Liu, Y. Kang, M. Zhang, X. Wang and D. Li, Self-sustained oscillation and cavitation characteristics of a jet in a Helmholtz resonator, *International Journal of Heat and Fluid Flow*, 68 (2017) 158-172.
[16] D. Li, Y. Kang, X. Ding, X. Wang and Z. Fang, Effects of nozzle inner surface roughness on the performance of self-resonating cavitating waterjets under different ambient pressures, *Strojniški vestnik-Journal of Mechanical Engineering*, 63 (2) (2017) 92-102.
[17] D. Li, Y. Kang, X. Ding, X. Wang and Z. Fang, An experimental investigation on the pressure characteristics of high speed self-resonating pulsed waterjets influenced by feeding pipe diameter, *Journal of Mechanical Science and Technology*, 30 (11) (2016) 4997-5007.
[18] D. Li, Y. Kang, X. Ding, X. Wang and Z. Fang, Effects of area discontinuity at nozzle inlet on the characteristics of high speed self-excited oscillation pulsed waterjets, *Experimental Thermal and Fluid Science*, 79 (2016) 254-265.
[19] D. Li, Y. Kang, X. Ding, X. Wang and W. Liu, Effects of feeding pipe diameter on the performance of a jet-driven Helmholtz oscillator generating pulsed waterjets, *Journal of Mechanical Science and Technology*, 31 (3) (2017) 1203-1212.
[20] D. Li, Y. Kang, X. Wang, X. Ding and Z. Fang, Effects of nozzle inner surface roughness on the cavitation erosion characteristics of high speed submerged jets, *Experimental Thermal and Fluid Science*, 74 (2016) 444-452.
[21] D. Li, Y. Kang, X. Ding, X. Wang and Z. Fang, Effects of area discontinuity at nozzle inlet on the characteristics of self-resonating cavitating waterjet, *Chinese Journal of Mechanical Engineering*, 29 (4) (2016) 813-824.
[22] D. Li, Y. Kang, X. Ding and W. Liu, Experimental study on the effects of feeding pipe diameter on the cavitation erosion performance of self-resonating cavitating waterjet, *Experimental Thermal and Fluid Science*, 82 (2017) 314-325.
[23] D. Li, Y. Kang, X. Ding and W. Liu, Effects of the geometry of impinging surface on the pressure oscillations of self-resonating pulsed waterjet, *Advances in Mechanical Engineering*, 9 (8) (2017) 1687814017720081.
[24] D. Li, X. Li, Y. Kang, X. Wang, X. Long and S. Wu, Experimental investigation on the influence of internal surface roughness of organ-pipe nozzle on the characteristics of high speed jet, *Journal of Mechanical Engineering*, 51 (17) (2015) 169-176 (in Chinese).
[25] Z. Fang, Y. Kang, X. Wang, D. Li, Y. Hu, M. Huang and X. Wang, Numerical and experimental investigation on flow field characteristics of organ pipe nozzle, *IOP Conference Series: Earth and Environmental Science*, IOP Publishing, 22 (5) (2014) 052020.
[26] S. Crow and F. Champagne, Orderly structure in jet turbulence, *Journal of Fluid Mechanics*, 48 (3) (1971) 547-591.
[27] G. Li, Z. Shen, C. Zhou, D. Zhang and H. Chen, Investigation and application of self-resonating cavitating water jet in petroleum engineering, *Petroleum Science and Technology*, 23 (1) (2005) 1-15.

Deng Li received his B.S. and Ph.D. degrees from Wuhan University, China, in 2012, and 2017. He is now doing postdoctoral research at Huazhong University of Science and Technology, China.